Materials Science & Engineering A 890 (2024) 145935

Contents lists available at ScienceDirect

Materials Science & Engineering A

journal homepage: www.elsevier.com/locate/msea

Design rules to develop solute lean α+β titanium alloys exhibiting high work-hardening by reorientation induced plasticity

O. Dumas [a,b,*], L. Malet [a], P. Kwaśniak [c], F. Prima [b], S. Godet [a]

[a] 4MAT, Université Libre de Bruxelles, 50 Avenue F.D. Roosevelt (CP 165/63), 1050, Bruxelles, Belgium
[b] PSL Research University, Chimie ParisTech, CNRS, Institut de Recherche de Chimie Paris, 75005, Paris, France
[c] Center of Digital Science and Technology, Cardinal Stefan Wyszynski University in Warsaw, Warsaw, Poland

ARTICLE INFO

Keywords:
Titanium
Work-hardening
Dual-phase
Martensite
Reorientation induced plasticity
Alloy design

ABSTRACT

While work-hardening is typically considered in Ti as a prerogative of the β-metastable alloys, this paper introduces a novel perspective, presenting a set of alloy design rules to develop solute lean α + β titanium alloys exhibiting increased work-hardening capabilities. More specifically, reaching this goal is made possible through the development of α + α′ microstructures exhibiting Reorientation Induced Plasticity (RIP) within the α′ martensitic phase. The microstructural requirements for activating RIP and maximizing mechanical properties (i.e., combining high work-hardening, yield strength and ductility levels) are derived from an analysis of the microstructures/mechanical property relationships of various α + α′ samples. A set of design rules is provided. Emphasis is laid on the pivotal role of the chemistry of the α′ martensitic phase in RIP activation and a Molybdenum equivalent chemical criterion is proposed. The α phase is here suggested as a mean to reduce the prior β grain size and the resulting size of the martensite plates. This approach reveals that the versatile thermal treatments leading to α+α' structures broaden the mechanical property landscape, achieving large work-hardening capabilities (typically over 500 MPa) that can be combined with high yield strength (over 800 MPa).

1. Introduction

Titanium alloys, especially Ti-6Al-4V, have experienced unprecedent growth in their use in widely differing fields, from biomedical devices to aerospace applications [1,2]. Of particular relevance for aircraft industry usage, Ti-6Al-4V α+β bimodal microstructures, consisting of a mixture of primary, equiaxed alpha (α) nodules and secondary, intragranular lamellar α phase, are the results of complex thermo-mechanical schemes designed after decades of optimization for yield strength and fatigue resistance levels [3]. However, the plastic behavior of conventional titanium alloys still limits their potential use in other advanced applications when compared to steels [4]. They usually display low work-hardening capabilities (typically around 150 MPa in Ti-6Al-4V [5]), bringing subsequent limited ductility level and rapid strain localization. The ability to resist localized deformation, which is reflected by the achievement of large ductility level, is indeed primarily due to the capacity of the material to work-harden [6,7].

In this regard, the so-called β-metastable titanium alloys stand well above the other titanium alloys thanks to the occurrence of "alternative" plastic deformation mechanisms which add up to classical dislocation glide: TRansformation Induced Plasticity (TRIP) and/or TWinning Induced Plasticity (TWIP) [8–10]. The simultaneous occurrence of these multiple deformation mechanisms greatly enhances the work-hardening capabilities (typically around 500 MPa for Ti-12Mo [8]) through the generation of a dynamic Hall-Petch effect and a marked mechanical contrast between the mechanical twins and the surrounding matrix. For such alloys, the design approach has mostly consisted in establishing a relationship between the chemical composition of the β phase and its mechanical stability/instability [11–13]. The β phase must indeed undergo a controlled "chemical destabilization", i.e., it should be sufficiently depleted in β-stabilizer elements and/or enriched in α-stabilizer elements so as to enter a compositional region of mechanical instability, which, once reached, promotes the occurrence of "alternative" deformation mechanisms. This approach is usually rationalized using Bo (Bond-Order)/Md (Metal d orbital energy level) phase stability maps [11–13]. However, in the majority of the developed TRIP/TWIP alloys, the increase in the work-hardening capabilities comes almost always with a limited yield strength (typically around 500 MPa) that can be attributed to the moderate triggering stress for the TRIP/TWIP effects [8]. Various strategies have been and are still currently being explored

* Corresponding author. 4MAT, Université Libre de Bruxelles, 50 Avenue F.D. Roosevelt (CP 165/63), 1050, Bruxelles, Belgium.
E-mail address: odeline.dumas@hotmail.fr (O. Dumas).

https://doi.org/10.1016/j.msea.2023.145935
Received 9 October 2023; Received in revised form 14 November 2023; Accepted 20 November 2023
Available online 23 November 2023
0921-5093/© 2023 Elsevier B.V. All rights reserved.

to tackle this issue: trying to take advantages of the Hall-Petch effect [14, 15], solid solution strengthening [16,17] or precipitation strengthening [18–20]. While quite effective, these strategies still fall short of the typical aeronautical standards that require reaching a yield strength of about 900 MPa [21]. Furthermore, the β-metastable titanium alloys inherently necessitate large amount of often costly alloying elements (Mo, Ni, V, …) and this, in turn, calls for the necessity to foster the development of leaner alloys that are not only cheaper but also more easily recyclable. Hence there is a clear need to develop cost-effective, solute lean α+β Ti alloys combining a high strength together with high work-hardening capabilities. This opportunity is well illustrated in Fig. 1, where the yield strength of various Ti alloys is plotted as a function of their work-hardening (defined as the difference between the UTS and the yield strength (σ_y)). A clear opportunity space is there defined.

Recently, it was shown that the work-hardening capabilities of Ti-6Al-4V can be significantly enhanced by substituting the lamellar α phase of the classical α+β bimodal microstructure by martensite (α′) leading to a so-called α + α' 'dual-phase' microstructure [22]. It consists of a mixture of V-lean and Al-rich α phase and V-rich and Al-lean α′ hexagonal martensite (since α′ inherits the chemical composition of the "high temperature" parent β phase that is enriched in β-stabilizers elements). Pragmatically, this resumes to substitute air cooling for water quenching in the last step of the conventional heat treatments. Such rather subtle modification of the microstructure turns out to improve significantly the work-hardening capabilities of Ti-6Al-4V (around 300 MPa) while keeping a high yield strength (nearly 900 MPa) [22].

In this first analysis, the enhanced work-hardening behavior has been attributed to the mechanical contrast between the two phases, with α′ martensite being the most ductile phase [23]. In a very recent study, a thorough EBSD analysis at the scale of the α′ martensite evidenced that during deformation, the martensite was undergoing a massive reorientation with specific variants growing at the expense of others [24,25]. This phenomenon was designated as Reorientation Induced Plasticity or RIP effect [25,26]. The crystallography and underlying rules have been thoroughly examined and rationalized [24,25]. Notably, it was shown that when the α′ martensite undergoes crystallographic reorientation, the martensitic variant whose transformation strain complies best with the applied stress (called "favored") grows at the expense of the other variants (called "unfavored"). This growth is thought to occur through the motion of the specific and mobile intervariant interface plane associated with the $[4\bar{5}1\bar{3}]_{\alpha'}$ Type II twin. Consequently, the orientation of the favored variant replaces the orientations of the unfavored variants, inducing a massive reorientation of the martensitic middle. The remarkable increase in work-hardening in Ti-6Al-4V through α + α' microstructures exhibiting RIP is also presented in Fig. 1.

In the following, based on the existing opportunity space of Fig. 1, Reorientation Induced Plasticity into an α′ hexagonal martensite is proposed to achieve unprecedented product of yield strength and work-hardening. In the case of RIP-assisted α+β alloys, design considerations are, so far, absent from any scientific discussions despite the clear fact that the presence of an α′ hexagonal martensite is obviously insufficient for the occurrence of RIP upon deformation (as demonstrated unambiguously in Ti-6Al-4V). Consequently, there is a pressing need for a more systematic approach to design principles in the development of optimized RIP-assisted α+β alloys. This involves, firstly, introducing basic design principles based on a "phase by phase" investigation with a focus on both chemical and microstructural aspects. Subsequently, a more specific discussion based on both α′ martensite underlying chemistry (drastically depending on the thermal path for a given alloy) and microstructures is then developed on validated RIP-based α+β alloys. The primary goal is to propose an initial set of fundamental design principles to streamline the rules governing the efficient development α+β RIP-assisted alloys to successfully obtain never-reached strength/work-hardening balance in this family of alloys. To do so, previously studied RIP-assisted alloys, namely Ti-6Al-4V and Ti-4.5Al-2.5F-0.25Si (TAFS) alloys, are first re-used to evidence the existence of a chemical threshold for RIP occurrence in α' martensite and to derive microstructural design rules to maximize the product of strength and work-hardening. Then, two different Ti-alloys are produced based on those requirements and tested under uniaxial tension to assess the effectiveness of the proposed design strategy.

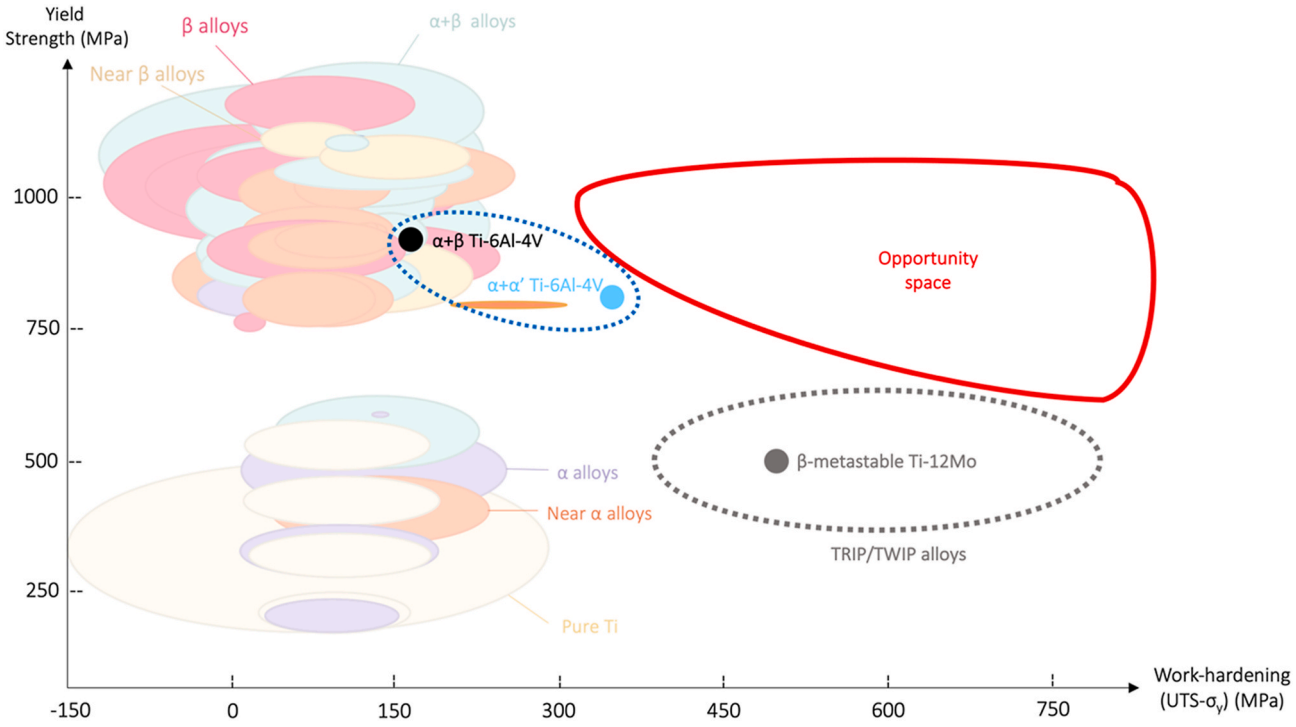

Fig. 1. Tensile strength (σ_y) of Ti alloys VS work-hardening ($\Delta\sigma$): a view of the spaces that are currently filled by titanium alloys and identification of an opportunity space aimed to reach.

2. Materials and methods

The production, thermo-mechanical processing and the chemical and microstructural characterization of Ti-6Al-4V and Ti-4.5Al-2.5Fe-0.25Si alloys were thoroughly described in Refs. [24,25]. Based on design criterion that will be derived in the following, two Ti-alloys were produced by plasma arc melting as 60 g ingots by plasma arc melting. The first one exhibits the same chemical composition as the commercially available Ti-4Al-4Mo-4Sn-0.5Si (Ti551) alloy while the second is a Ti-6Al-8V alloy i.e., a vanadium enriched version of the classical Ti-6Al-4V alloy. The ingots were subsequently heat-treated during 5 min at 1020 °C followed by water quench and then hot-rolled in the α+β field at a temperature of 770 °C.

Rectangular specimens (gauge length of 30 mm, width of 6 mm and thickness about 1.1 mm) were machined from the hot-rolled sheets. The specimens were encapsulated into quartz tubes filled with argon to perform annealing treatments at different temperatures in the α+β field (i.e., sub-transus) during 1h followed by quenching in water by breaking the capsules to generate α+α' microstructures while limiting oxidation. The β-transus temperatures of Ti-6Al-8V and Ti-551 were computed as 945 °C and 1000 °C, respectively (computed by TIMET internal database).

Then, the specimens were chemically polished using a solution composed of 80 % distilled water, 10 % Hydrofluoric acid and 10 % Nitric acid to remove the oxidation layer induced by the hot-rolling step and the annealing heat treatment (300 μm on each side).

Conventional and ex-situ tensile tests were performed at a cross head speed of $5.10^{-4}s^{-1}$ using a universal Zwick Roell Z100 tensile testing machine.

For EBSD analysis, samples were electro-polished in a solution of 95 % methanol and 5 % Sulfuric acid at -50 °C using a voltage of 20 V.

Phase proportion have been determined from BSE images using ImageJ software. BSE images have been carried out on a ZEISS LEO 1530 FEG-SEM operated at 20 kV.

EBSD measurements were performed on a Hitachi SU70 FEG-SEM operated at 15 kV and equipped with a Hikari® CCD camera. A step size of 40 nm was used. EBSD patterns were post-processed using EMSphInx software, an EBSD indexing algorithm based on spherical harmonic transforms [27]. The analysis of the EBSD measurements was carried out using TSL® OIM analysis™ software.

Thin foils for TEM examination were mechanically ground down to a thickness of about 80 μm. 3 mm diameter discs punched from this plate were further electro-polished by the twin-jet method using a solution containing 95 % of methanol and 5 % of sulfuric acid at 20 V and −40 °C. The chemical compositions of the individual phases were measured using a XFlash® 6T | 60 Bruker EDX system attached to a Tecnai G2 20 S-TWIN TEM operated at 200 kV.

3. Results and discussion

3.1. Chemistry governs the occurrence of reorientation

Fig. 2 are Inverse Pole Figure (IPF) EBSD maps of the α′ martensite of Ti-6Al-4V α + α' 'dual-phase' microstructures annealed at 880 °C (a) and 920 °C (b.) after deformation (post-mortem). The α phase has been removed so as to focus on the α′ martensite. Profuse reorientation is evidenced in the α′ martensite of 880 °C while it is totally absent in 920 °C sample. One of the main parameters that is influenced by the change in the annealing temperature is the chemical composition of the α′ martensite. These compositions are given for 880 °C and 920 °C samples in Fig. 2. The 880 °C sample, the α′ martensite is enriched in V and depleted in Al. Indeed, at lower annealing temperatures, the partitioning of the β-stabilizing element into the high temperature parent β phase implies that the daughter α′ martensite chemistry goes away from the nominal composition of the alloy. Note that the combined effect of various β-stabilizing elements is usually estimated using the empirical Mo_{eq}[1] parameter (in which α-stabilizers are counted as negative). In the α′ martensite of the 880 °C sample, the partitioning of the alloying elements is such that Mo_{eq} increases so as to reach precisely the value of 0 (Fig. 2). Of prime importance, this result suggests that, similarly to the β-metastable alloys, the occurrence of reorientation in the hcp α′ martensite is strongly chemistry dependent. More precisely, it appears that reorientation is triggered when the hcp α′ martensite phase is "mechanically destabilized", and that the chemical threshold for the onset of this destabilization corresponds to $Mo_{eq} \geq 0$. Pragmatically, it means that, for the reorientation to occur, the hcp α′ martensite phase has to be sufficiently enriched in β-stabilizing elements and/or depleted in α-stabilizing elements (rather than the bcc β phase being destabilized in β-metastable alloys). As a fact, in the cases where Mo_{eq} value is negative, typically in the case of the 920 °C sample (Fig. 2), the α-stabilizers elements may play an excessive stabilizing role in the hcp α′ martensite which, then, cannot undergo the reorientation process. However, it should be carefully noted as well that the value of Mo_{eq} equal to 0 is derived empirically on the Ti-6Al-4V α + β alloy, i.e., it has been defined for an alloy where both β-stabilizing (with positive coefficients in the Mo_{eq} formula) and α-stabilizing (with negative coefficients in the Mo_{eq} formula) coexist. From the particular case of Ti-6Al-4V, it is postulated as a general design rule that reorientation will occur in α′ martensite whenever its chemical composition ensures $Mo_{eq} \geq 0$. The soundness of this empirical rule will be strengthened in this study.

3.2. Reorientation as a key deformation mechanism to increase work-hardening

Fig. 3 gathers the engineering tensile curves (a.) and work-hardening rate curves (b.) of Ti-6Al-4V α + α' 'dual-phase' microstructures annealed at 880 °C and 920 °C respectively and compared to a classical Ti-6Al-4V α + β bimodal microstructure used as the reference. It shows that the occurrence of reorientation is concomitant with a drastic change in the mechanical properties. More precisely, although the yield strength of 880 °C is lower than 920 °C (but stay close to the reference), it shows both a superior work-hardening and ductility. The improvement in the work hardening capabilities in the 880 °C sample can be better appreciated in the work-hardening rate curves (Fig. 3b) with the 920 °C sample reaching Considere's criterion at low strain level while the uniform strain is almost doubled in the 880 °C sample reaching more than 11%. From what precedes, it can be hypothesized that enabling reorientation induced plasticity (RIP) in the α′ martensite has the potential to increase substantially the work-hardening capabilities of the alloy. However, it is important to keep in mind that other microstructural features differ slightly between the 880 °C and 920 °C samples. For example, the fraction of the α phase is higher in 880 °C sample (63 ± 1% in 880 °C sample compared to 56 ± 1% in 920 °C sample). This result alone is therefore not sufficient to understand the relative role of the α phase and of the RIP effect on the work-hardening capabilities. In order to properly isolate the role of the RIP effect, a fully martensitic microstructure whose nominal chemical composition respects the criterion $Mo_{eq} \geq 0$ is investigated. It corresponds to the composition of α′ in the α+α′ 880 °C sample.

Consequently, an ingot with nominal composition Ti-4.6Al-6.8V, has been produced by plasma arc melting. This ingot has then been hot-

[1] Mo_{eq} = 1.0(wt% Mo) + 0.28(wt% Nb) + 0.22(wt% Ta) + 0.67(wt% V) + 1.60(wt% Cr) + 2.90(wt% Fe) + 0.44 (wt% W) + 1.25(wt% Ni) + 1.70(wt% Mn) + 1.70(wt% Co) – 1.0(wt% Al) [28].

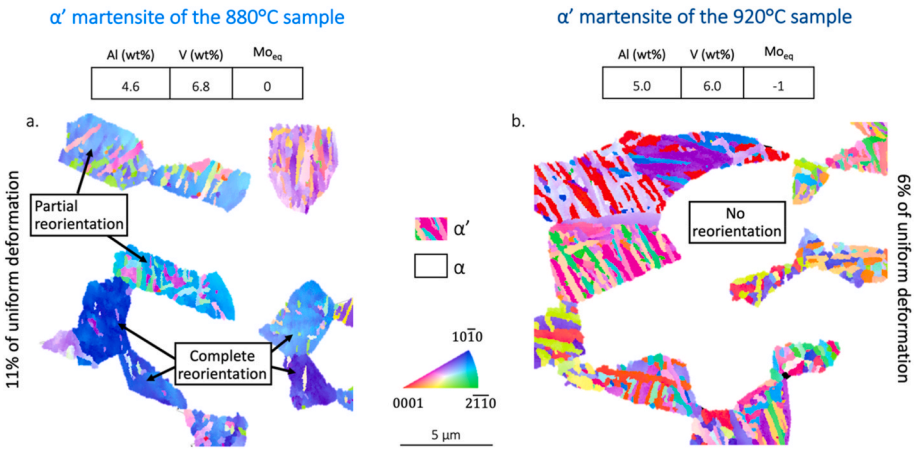

Fig. 2. Inverse Pole Figure (IPF) EBSD maps of the α′ martensitic phase after deformation (post-mortem analysis) of Ti-6Al-4V samples annealed at 880 °C (a.) and 920 °C (b.).

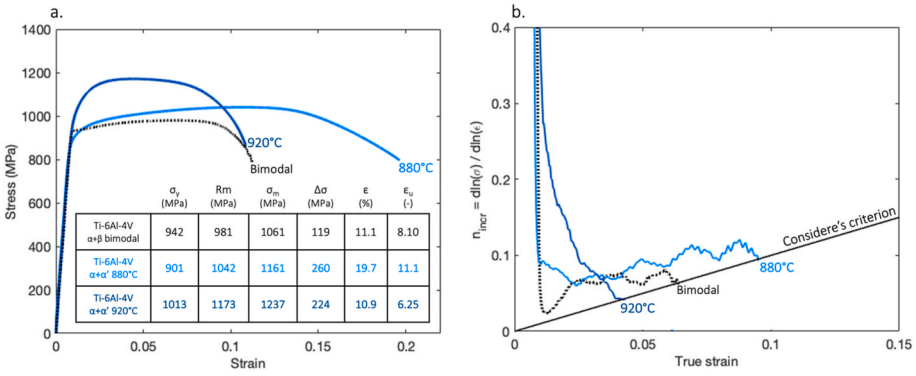

Fig. 3. a. Engineering tensile curves and b. work-hardening rate curves of the Ti-6Al-4V 880 °C, 920 °C and bimodal (reference) samples.

rolled at 770 °C, heat-treated during 5 min at 1020 °C (above the β-transus temperature) and then water quenched to produce a fully martensitic microstructure. Fig. 4 a is the IPF EBSD map of this sample after deformation and Fig. 4 b is the corresponding engineering tensile curve. Intense reorientation is shown to occur. It goes along with high work-hardening capabilities, more than two times larger than for the reference bimodal structure. It confirms that the *criterion* $Mo_{eq} \geq 0$ *enables the reorientation* of the martensite and foremost, it validates that RIP effect is sufficient on its own to improve the work-hardening capabilities of the alloy. A detailed discussion of how RIP can contribute to work-hardening can be found in Ref. [25].

It is however important to notice that this fully martensitic microstructure exhibits a very limited ductility compared to the dual-phase samples. This suggests that, in some way or another, the presence of the α phase plays an important role regarding the ductility. One of the objectives of the next section is to rationalize the role of the α phase.

3.3. Microstructure-based rules to enhance the strength ductility balance

To emphasize the importance of the α phase on ductility, we refer to

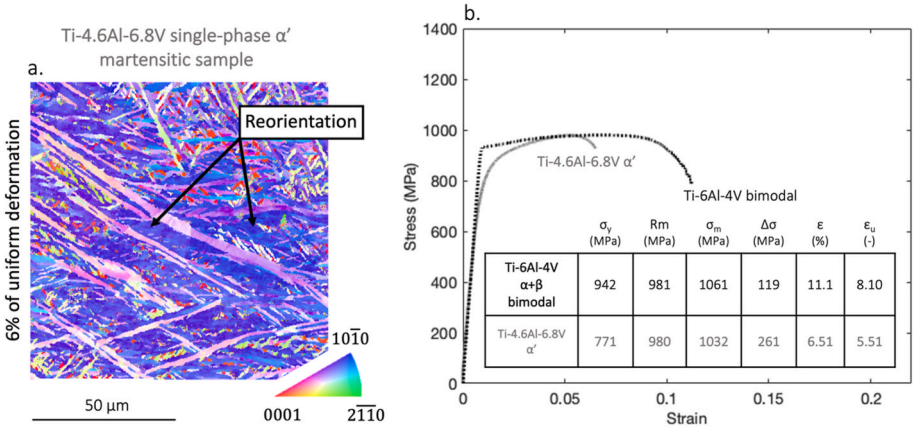

Fig. 4. a. IPF map after deformation of Ti-4.6Al-6.8V single-phase α′ martensite sample and b. Engineering tensile curves of theTi-4.6Al-6.8V single-phase α′ martensite sample and of the Ti-6Al-4V bimodal (reference) sample.

previously published results [25] on Ti-4.5Al-2.5Fe-0.25Si α + β titanium alloy whose nominal Mo_{eq} is 2.75, respecting $Mo_{eq} \geq 0$. The alloy was first water quenched from 1000 °C (above the β-transus) to obtain a fully martensitic microstructure and Fig. 5a and b shows the engineering tensile curve and work-hardening curve of this specimen, respectively. This Ti-4.5Al-2.5Fe-0.25Si (TAFS) single-phase martensite displays improved work-hardening capabilities compared to Ti-4.6Al-6.8V single-phase martensite, thereby assessing definitely the pivotal role of reorientation in reaching efficiently high work-hardening capabilities. However, the ductility is very limited. In fact, the sample even *breaks* before reaching Considere's criterion (Fig. 5b), suggesting premature damaging of the specimen. This behavior is believed to arise from the very rapid growth of the parent β grains during the heat treatment above the β-transus [29]. Indeed, the martensitic transformation occurs sequentially in large parent β grains [30]. More precisely, a first generation of very large α′ plates whose length scales with the size of the parent β grains will form upon quenching and then a second generation of much smaller plates grow (at a lower temperature) inside the pocket left untransformed by the first generation of variant. This is much different from the transformation occurring in smaller β grains (typically in Ti-6Al-4V 880 °C sample) since in that case only one generation of rather small plates is able to form [24]. In the case of large β grains, deformation preferentially takes place within the largest plates due to their strength difference with the neighboring smaller plates. This results in the formation and coalescence of micro-voids in these large plates results in a so-called macroscopic "pseudo-brittle" fracture [31]. The effect is well-documented in literature and it is clearly stressed that large martensite plates are to be avoided [31,32]. When large martensite laths are present, the intrinsic capacity of the martensite to strain-harden by reorientation was not sufficient to compensate the local stress increase, leading inevitably to an early fracture. It therefore appears that to fully take advantage of the potential of reorientation, it is mandatory to limit the size of the martensite plates by preventing the growth of the parent β grains. A common way to achieve this goal in industrial practice is to make use of the pining effect of the α phase. This naturally leads to another design rule stating that the annealing treatment should occur *below the β-transus* so as to generate α+α′ dual phase microstructures instead of α′ alone.

The remaining question is to determine the fraction of α phase that optimizes the mechanical properties, i.e., the fraction that maximizes the product of yield strength and work-hardening. In this regard, several annealing temperatures between 920 °C (25 % of α phase) and 950 °C (10% of α phase) were investigated in the Ti-4.5Al-2.5Fe-0.25Si alloy. The corresponding tensile curves are shown in Fig. 6. All the samples now reach Considere's criterion thereby confirming the validity of the previously stated criterion. Furthermore, decreasing the annealing temperature from 950° to 920 °C improves the work-hardening but this gain comes along with a substantial decrease in the yield strength level. As such, the 950 °C sample containing a fairly low amount of α phase combines a high yield strength of 905 MPa (equating the standards of Ti-6Al-4V) with a very high work-hardening of 515 MPa; a value that is usually obtained only in β-metastable alloy [4]. The important information behind this result is that RIP effect, more than ensuring high work-hardening rates, allows to take up the big challenge of combining it to high yield strength when the quenching temperature is maximized. From this result, a new and last design rule is proposed that states that the *annealing temperature should be chosen as close as possible but below the β-transus temperature*. This way, the fraction of α′ martensite is maximized so as to increase the yield strength and the presence of a small amount of α phase prevents the "explosive" growth of the β grains and the associated premature failure.

3.4. Design rules

From the above empirical findings, the following alloy design rules are proposed to develop solute lean titanium alloys exhibiting work-hardening by Reorientation Induced Plasticity:

- α + β alloys should be targeted so as to be able to generate α' + α microstructures by heat treatments and to ensure solute leanness. It can indeed be considered that α + β alloys are dilute compared to β-metastable alloys.
- The composition of the α′ should be such that its $Mo_{eq} \geq 0$ to trigger the reorientation of the α′ martensitic phase and to unlock the work-hardening capabilities. It means that a certain level of chemical destabilization is required in the hexagonal α′ martensite to expect efficient RIP effect for superior work-hardening.
- The β grain size should be limited and hence consequently that of the martensite plates by making use of the pining effect of the α phase. This condition implies to realize subtransus heat-treatments to generate α' + α phases rather than super-transus heat-treatments leading to α′ alone. However, the amount of the α should be kept at a minimum so as to maximize the yield strength while keeping a good work-hardening level. Stated otherwise the annealing treatment should be performed below but as close as possible to the β-transus temperature.

3.5. Applying the design rules to other titanium alloys

In the rest of the present paper, these rules are applied to 2 different α + β alloys to demonstrate the effectiveness of the present alloy design strategy in extending the landscape in the space of titanium alloys with improved work-hardening capabilities. The mechanical properties and the deformation mechanisms of the materials obtained through the design strategy are studied, and some perspectives are proposed.

2 α + β alloys were selected to challenge the proposed design

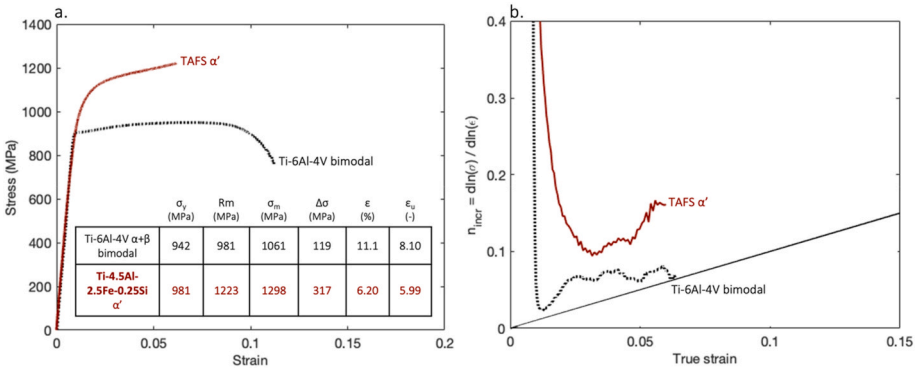

Fig. 5. a. Engineering tensile curves and b. work-hardening curves of the Ti-4.5Al-2.5Fe-0.25Si single-phase α′ martensite sample and of the Ti-6Al-4V bimodal (reference) sample.

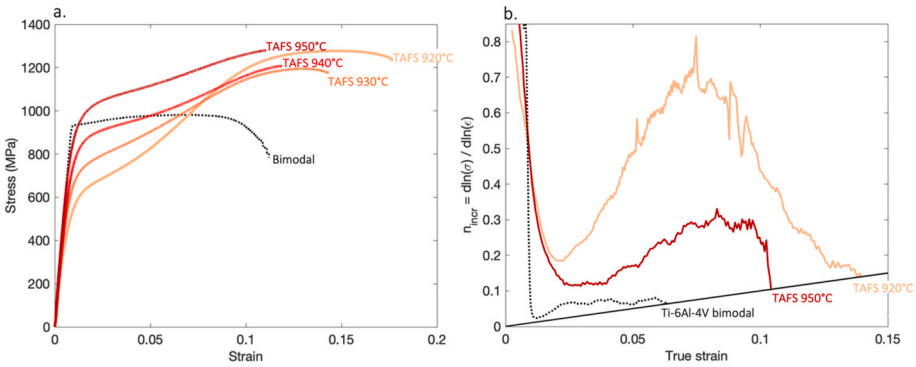

	σ_y (MPa)	Rm (MPa)	σ_m (MPa)	$\Delta\sigma$ (MPa)	ε (%)	ε_u (-)
Ti-6Al-4V α+β bimodal	942	981	1061	119	11.1	8.10
TAFS α+α′ 920	585	1233	1478	893	17.7	15.1
TAFS α+α′ 930	670	1195	1354	684	14.3	12.7
TAFS α+α′ 940	769	1207	1350	581	12.7	11.2
TAFS α+α′ 950	905	1278	1420	515	11.9	10.5

Fig. 6. Engineering tensile curves and b. work-hardening curves of the Ti-4.5Al-2.5Fe-0.25Si samples heat-treated at 920, 930, 940 and 950 °C and of the Ti-6Al-4V bimodal (reference) sample.

strategy:

- Ti-6Al-8V which is a modified Ti-6Al-4V with twice as much V content. The aim is to increase the Mo_{eq} of the martensite phase to increase its mechanical instability and thus, enhance the RIP effect. In its nominal composition, the Mo_{eq} value is -0.6. For this alloy, an annealing temperature of 920 °C (very close to the β transus of 945 °C) was chosen so as to generate an α+α′ microstructure with a very small amount of α. This allows the martensite to reach a Mo_{eq} = 0.5 (Table 1) respecting $Mo_{eq} \geq 0$ thanks to the partitioning of the alloying elements.
- Ti-4Al-4Mo-4Sn-0.5Si (Ti-551), an industrial alloy known for its high strength [33]. In its nominal composition, Mo_{eq} equals 0.0. An annealing temperature of 950 °C (very close to the β transus of 1000 °C) was chosen. This allows the martensite to reach a Mo_{eq} of 1.7. To further verify the validity of the design rules, another annealing temperature of 920 °C was chosen. This allows the martensite to reach a Mo_{eq} = 4.

Fig. 7 shows the systematic and profuse occurrence of reorientation in the martensite of the selected alloys heat-treated following the design rules. Indeed, whereas the martensites display before deformation well-defined plates with different crystallographic orientations, nearly a unique orientation close to $(10\bar{1}0)_{\alpha}$ remains after deformation as it has grown at the expense of the other martensite plates packets by reorientation. For a more detail description and rationalization of such phenomena, the readers is referred to Refs. [24,25]. For further insights into the assessment of the crystallographic nature of martensite, whether hexagonal or orthorhombic, readers are directed to Ref. [34].

The engineering and true stress/strain curves as well as the work-hardening rate curves of the selected alloys heat-treated following the design rules in Fig. 8 a,b and d and are compared to Ti-6Al-4V alloy exhibiting a conventional α + β bimodal microstructure. The main mechanical properties are summarized in Fig. 8 c.

These results prove that the design strategy is very effective, as the 2 alloys consistently exhibit work-hardening that are 4.5 to 6.3 times larger than in conventional Ti-6Al-4V. The ductility levels measured by the fracture strains are excellent, as they are superior to that of conventional Ti-6Al-4V. In particular, they are all superior to the 10% at fracture required by aeronautic standards [21]. Even more important, as a result of the improved work-hardening capabilities, the uniform strains reach 13-15%, compared to 8% for the reference bimodal Ti-Al6-V4 microstructure. The 'bump' in the hardening curve correlates well with the very large work hardening levels of the tensile curves.

Comparison between the Ti-551 920 °C and 950 °C samples confirms that the yield strength is increased when the annealing temperature is increased and chosen right below the β-transus. Following the design rules is however not sufficient to ensure a high yield strength level comparable to the bimodal structures as it is achieved by the TAFS 950 °C sample (Fig. 6a). The microstructures of the TAFS 950 °C, Ti-551 950 °C and Ti-6Al-8V 920 °C samples are very similar. Indeed, their martensite volume fraction is maximized by applying an annealing temperature right below β-transus and they verify the criterion $Mo_{eq} \geq 0$. However, the yield strength of the TAFS 950 °C is 150 MPa higher than that of the two other alloys. It means that the nature of the alloying elements plays a crucial role in the strength of the alloy, and this opens a promising field of investigation.

Table 1
Chemical compositions and Mo_{eq} of the α' martensite of the heat-treated samples.

Alloy/T°C	Chemical content of the α′ martensite (wt%)				Mo_{eq}
Ti-6Al-8V	Al		V		
920	5.5		9.0		0.5
Ti-551	Al	Mo	Sn	Si	
920	2.0	6.0	4.5	0.3	**4.0**
950	2.9	4.6	4.2	0.4	**1.7**

4. Conclusions: from opportunity to reality

The mechanical properties of all the newly developed microstructures can now be placed within the landscape σ_y versus $\Delta\sigma$ of titanium alloys. This is presented in Fig. 9 and shows that the proposed design strategy was very efficient at least for two reasons. First, it proves that reaching high work-hardening capabilities is not a prerogative of the β-metastable alloys, as it can be extended to a large family of cost-effective α + β alloys through the activation of RIP effect into the α′

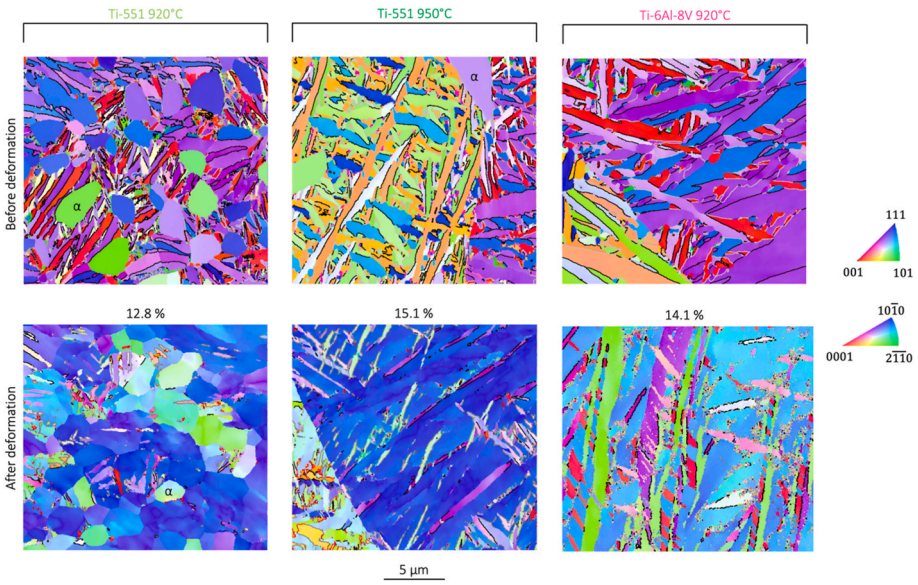

Fig. 7. IPF EBSD maps before and after deformation of Ti-68 and Ti-551 alloys exhibiting α+α′ microstructures for different annealing temperatures. 920 °C for Ti-68, 920 °C and 950 °C for Ti-551.

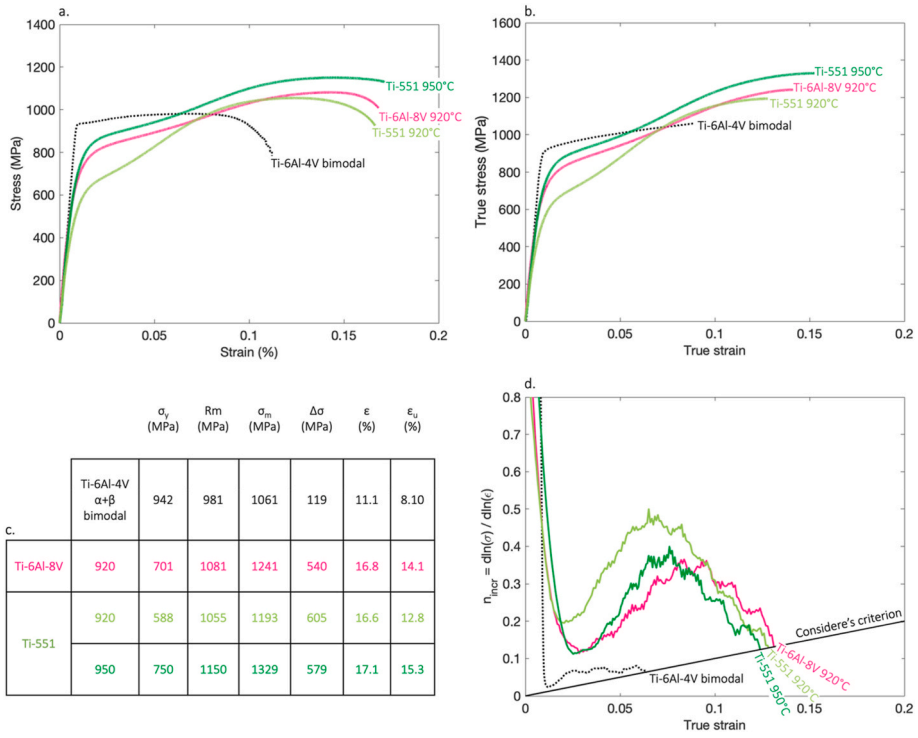

c.

	α_y (MPa)	Rm (MPa)	σ_m (MPa)	Δσ (MPa)	ε (%)	ε_u (%)
Ti-6Al-4V α+β bimodal	942	981	1061	119	11.1	8.10
Ti-6Al-8V	920	701	1081	1241	540	16.8	14.1
Ti-551	920	588	1055	1193	605	16.6	12.8
	950	750	1150	1329	579	17.1	15.3

Fig. 8. a. Engineering and b. true stress/strain curves and d. the work-hardening rate curve of the Ti-6Al-8V, Ti-551, TA2.5FS samples exhibiting α+α′ microstructures and Ti-6Al-4V exhibiting a conventional bimodal microstructure, c. Table gathering the yield strength (σ_y), engineering ultimate tensile strength (R_m), maximum true strength (σ_m), the work-hardening ability which is defined as the difference between the maximum true strength and the yield strength ($\Delta\sigma$), the engineering strain to fracture (ε) and true uniform strain (ε_u).

martensitic phase. Mechanical instability can also be reached in solute lean α + β alloys to trigger Reorientation Induced Plasticity (RIP) effect leading to work-hardening capabilities comparable, if not superior, to those of β-metastable alloys. A necessary condition for the occurrence of RIP is that the Mo_{eq} of α' has to be superior or equal to 0.

Second, it shows that α + β alloys deforming by RIP further extend the landscape in the space of titanium alloys, as some alloys have reached the opportunity space. RIP is a highly versatile deformation mechanism whose effect on the mechanical properties sharply changes according to the microstructural features, allowing to access a wide range of mechanical properties. In particular, it allows to combine high yield strength and work-hardening, two properties which are usually found to be mutually exclusive, when the annealing temperature to generate α+α' microstructure is chosen right below the β-transus temperature. In particular, TAFS exhibits outstanding mechanical properties when heat treated at 950 °C which meets the requirements $\sigma_y \geq 900$ MPa

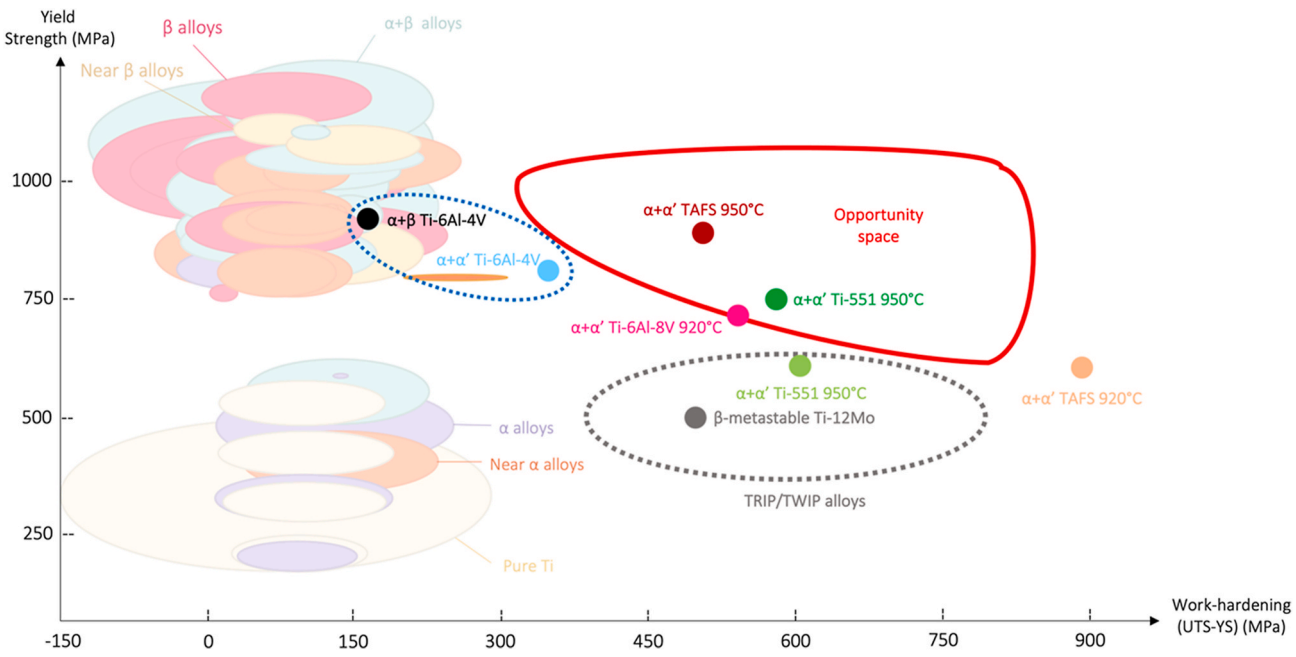

Fig. 9. Tensile strength (σ_y) of Ti alloys versus work-hardening ($\Delta\sigma$): comparison of the different results presented in the present paper.

and $\varepsilon \geq 10$ % required by aeronautic standards [21] while its work-hardening is 4.3 times higher than conventional bimodal Ti-6Al-4V. Further work includes the development of approaches to separate the effects of the numerous microstructural features on RIP effect and its subsequent influence on work-hardening and yield strength.

CRediT authorship contribution statement

O. Dumas: Conceptualization, Validation, Formal analysis, Investigation, Writing – original draft, Writing – review & editing, Visualization. **L. Malet:** Conceptualization, Validation, Writing – review & editing, Visualization, Supervision. **P. Kwaśniak:** Conceptualization, Writing – review & editing. **F. Prima:** Conceptualization, Validation, Writing – review & editing, Visualization, Supervision, Project administration. **S. Godet:** Conceptualization, Validation, Writing – review & editing, Visualization, Supervision, Project administration.

Declaration of competing interest

The authors declare that they have no known competing financial interests or personal relationships that could have appeared to influence the work reported in this paper.

Data availability

No data was used for the research described in the article.

Acknowledgements

The authors are grateful to the F.N.RS, Belgium, for financing this research and to Yvon Millet and Timet Savoie for providing the material and for sharing fruitful discussions. The present work was also carried out in the framework of the Iawatha FEDER project. The authors are also grateful to Colin Aughet for machining tensile test specimens and to Didier Robert for the preparation of some EBSD and TEM specimens.

References

[1] M. Peters, J. Kumpfert, C.H. Ward, C. Leyens, Titanium alloys for aerospace applications, Adv. Eng. Mater. 5 (6) (juin 2003) 419–427, https://doi.org/10.1002/adem.200310095.
[2] K. Wang, The use of titanium for medical applications in the USA, Mater. Sci. Eng., A 213 (1–2) (août 1996) 134–137, https://doi.org/10.1016/0921-5093(96)10243-4.
[3] C. Leyens, M. Peters, Titanium and Titanium Alloys: Fundamentals and Applications, Wiley-VCH Verlag GmbH & Co. KGaA, Weinheim, FRG, 2003, https://doi.org/10.1002/3527602119.
[4] R.K. Gupta, C. Mathew, P. Ramkumar, Strain hardening in aerospace alloys, Frontiers in Aerospace Engineering 4 (1) (2015) 1–13, https://doi.org/10.12783/fae.2015.0401.01.
[5] M. Donachie, Titanium: A Technical Guide, ASM International, 2000.
[6] N.K. Balliger, T. Gladman, Work hardening of dual-phase steels, Met. Sci. 15 (3) (mars 1981) 95–108, https://doi.org/10.1179/030634581790426615.
[7] M. Calcagnotto, D. Ponge, D. Raabe, Effect of grain refinement to 1μm on strength and toughness of dual-phase steels, Mater. Sci. Eng., A 527 (29–30) (nov. 2010) 7832–7840, https://doi.org/10.1016/j.msea.2010.08.062.
[8] C. Brozek, et al., A β-titanium alloy with extra high strain-hardening rate: design and mechanical properties, Scripta Mater. 114 (mars 2016) 60–64, https://doi.org/10.1016/j.scriptamat.2015.11.020.
[9] M. Marteleur, F. Sun, T. Gloriant, P. Vermaut, P.J. Jacques, F. Prima, On the design of new β-metastable titanium alloys with improved work hardening rate thanks to simultaneous TRIP and TWIP effects, Scripta Mater. 66 (10) (mai 2012) 749–752, https://doi.org/10.1016/j.scriptamat.2012.01.049.
[10] F. Sun, et al., A new titanium alloy with a combination of high strength, high strain hardening and improved ductility, Scripta Mater. 94 (2015) 17–20, https://doi.org/10.1016/j.scriptamat.2014.09.005, janv.
[11] M. Morinaga, Y. Murata, H. Yukawa, Alloy design based on the DV-Xα cluster method, in: H. Adachi, T. Mukoyama, J. Kawai (Eds.), Hartree-Fock-Slater Method for Materials Science 84, Springer-Verlag, Berlin/Heidelberg, 2006, pp. 23–48, https://doi.org/10.1007/3-540-31297-8_2.
[12] M. Abdel-Hady, K. Hinoshita, M. Morinaga, General approach to phase stability and elastic properties of β-type Ti-alloys using electronic parameters, Scripta Mater. 55 (5) (sept. 2006) 477–480, https://doi.org/10.1016/j.scriptamat.2006.04.022.
[13] D. Kuroda, M. Niinomi, M. Morinaga, Y. Kato, T. Yashiro, Design and mechanical properties of new i type titanium alloys for implant materials, Mater. Sci. Eng. 6 (1998).
[14] W.L. Wang, X.L. Wang, W. Mei, J. Sun, Role of grain size in tensile behavior in twinning-induced plasticity β Ti-20V-2Nb-2Zr alloy, Mater. Char. 120 (oct. 2016) 263–267, https://doi.org/10.1016/j.matchar.2016.09.016.
[15] S. Sadeghpour, S.M. Abbasi, M. Morakabati, L.P. Karjalainen, D.A. Porter, Effect of cold rolling and subsequent annealing on grain refinement of a beta titanium alloy showing stress-induced martensitic transformation, Mater. Sci. Eng., A 731 (juill. 2018) 465–478, https://doi.org/10.1016/j.msea.2018.06.050.
[16] Y. Danard, « Développement d'alliages de titane transformables par déformation: étude des relations microstructure/propriétés mécaniques », 2019.

[17] S. Sadeghpour, S.M. Abbasi, M. Morakabati, A. Kisko, L.P. Karjalainen, D.A. Porter, A new multi-element beta titanium alloy with a high yield strength exhibiting transformation and twinning induced plasticity effects, Scripta Mater. 145 (mars 2018) 104–108, https://doi.org/10.1016/j.scriptamat.2017.10.017.
[18] F. Sun, et al., Strengthening strategy for a ductile metastable β-titanium alloy using low-temperature aging, Materials Research Letters 5 (8) (nov. 2017) 547–553, https://doi.org/10.1080/21663831.2017.1350211.
[19] J. Gao, A.J. Knowles, D. Guan, W.M. Rainforth, ω phase strengthened 1.2GPa metastable β titanium alloy with high ductility, Scripta Mater. 162 (mars 2019) 77–81, https://doi.org/10.1016/j.scriptamat.2018.10.043.
[20] L. Lilensten, et al., From single phase to dual-phase TRIP-TWIP titanium alloys: design approach and properties, Materialia 12 (août 2020), 100700, https://doi.org/10.1016/j.mtla.2020.100700.
[21] SAE AMS 4928: titanium alloy bars, wire, forgings, rings, and drawn shapes 6Al-4V annealed, SAE International (7 décembre 2017).
[22] C. de Formanoir, et al., A strategy to improve the work-hardening behavior of Ti–6Al–4V parts produced by additive manufacturing, Materials Research Letters (oct. 2016) 1–8, https://doi.org/10.1080/21663831.2016.1245681.
[23] C. de Formanoir, et al., Micromechanical behavior and thermal stability of a dual-phase α+α' titanium alloy produced by additive manufacturing, Acta Mater. 162 (2019) 149–162, https://doi.org/10.1016/j.actamat.2018.09.050, janv.
[24] O. Dumas, L. Malet, B. Hary, F. Prima, S. Godet, Crystallography and reorientation mechanism upon deformation in the martensite of an α-α' Ti-6Al-4V dual-phase microstructure exhibiting high work-hardening rate, Acta Mater. 205 (2021), 116530, https://doi.org/10.1016/j.actamat.2020.116530 févr.
[25] O. Dumas, L. Malet, P. Kwaśniak, F. Prima, S. Godet, Reorientation Induced Plasticity (RIP) in high-strength titanium alloys: an insight into the underlying mechanisms and resulting mechanical properties, Acta Mater. (2022).
[26] S.W. Lee, J.M. Oh, J.H. Kim, C.H. Park, J.-K. Hong, J.-T. Yeom, Demonstration of martensite reorientation-induced plasticity by ultra-high strength titanium alloys, Mater. Sci. Eng., A (févr. 2021), 140878, https://doi.org/10.1016/j.msea.2021.140878.
[27] W.C. Lenthe, S. Singh, M.D. Graef, A spherical harmonic transform approach to the indexing of electron back-scattered diffraction patterns, Ultramicroscopy 207 (déc. 2019), 112841, https://doi.org/10.1016/j.ultramic.2019.112841.
[28] R. Kolli, A. Devaraj, A review of metastable beta titanium alloys, Metals 8 (7) (juin 2018) 506, https://doi.org/10.3390/met8070506.
[29] H. Beladi, Q. Chao, G.S. Rohrer, Variant selection and intervariant crystallographic planes distribution in martensite in a Ti–6Al–4V alloy, Acta Mater. 80 (nov. 2014) 478–489, https://doi.org/10.1016/j.actamat.2014.06.064.
[30] S. Banerjee, P. Mukhopadhyay, Martensitic transformations, Pergamon Materials Series 12 (2007) 257–376, https://doi.org/10.1016/S1470-1804(07)80057-5. Elsevier.
[31] A. Moridi, A. G. Demir, L. Caprio, A. J. Hart, B. Previtali, et B. M. Colosimo, « Deformation and Failure Mechanisms of Ti-6Al-4V as Built by Selective Laser Melting », p. 25.
[32] M. Ivasishin, M. Flower, et G. Lutjering, « Mechanisms of Martensite Formation and Tempering in Titanium Alloys and Their Relationship to Mechanical Property Development », Science and Technology, p. 16.
[33] G. Welsch, R. Boyer, E.W. Collings, Materials Properties Handbook: Titanium Alloys, ASM International, Materials Park, OH, 1994.
[34] O. Dumas, Work-hardening by "Reorientation Induced Plasticity" in Titanium Alloys: from a Fundamental Understanding in Ti-6Al-4V towards New Alloy Design Rules », Université Libre de Bruxelles et Chimie ParisTech, 2023.